



Starspot and flare activity – differences and similarities between stars with different inner structure

Bezovec 2023
Conference of Young Astronomers

Kamil Bicz
Astronomical Institute of the University of Wrocław

Table of contents

- Selected active fully convective M-type main-sequence stars
- Partially convective star CD-36 3202

BASSMAN

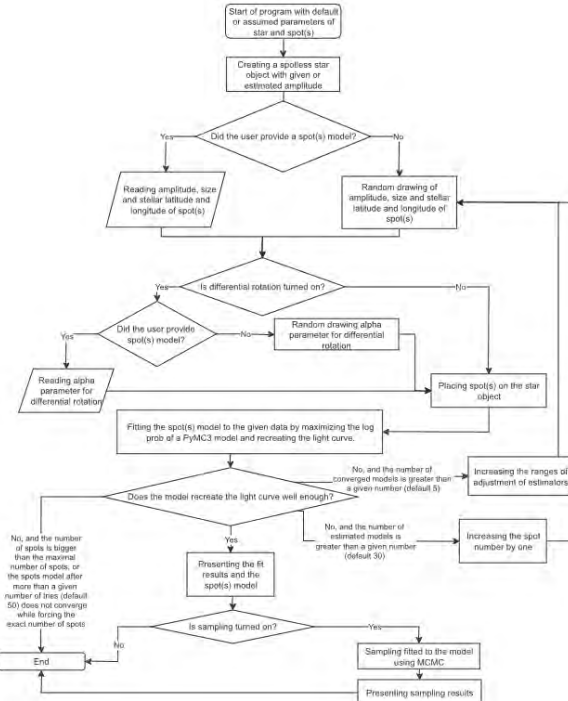


Figure 1. Flow diagram showing the operations of the BASSMAN software/program.

Bicz et al., 2022

Kamil Bicz, Astronomical Institute of the University of Wrocław

TIC ID = 273589987 HD = nan G208-42 Eruptive*

RA = 297.788835531591 [deg]

DEC = 46.4833913684977 [deg] Cygnus

Tmag = 10.2463 [mag] Terr = 0.0073089 [mag] DM = -5.0250 [mag]

SpType = M4.0V SpType_{B-V} = M2V_(Pecaut)

Parallax = 83.4814 [mas] Parallax err = 0.0365802 [mas] Dist = 11.9746 [parsec]

U = nan [mag] B = 14.61 [mag] V = 12.961 [mag] B-V = 1.649 [mag]

Teff = 3261.0 [K] Teff_{B-V} = 3582 [K]

log(g/[cm²s⁻²]) = 4.96237

Radius = 0.268565 [R_☉] Radius_{DM} = 0.310317 [R_☉]

Mass = 0.241211 [M_☉]

Density = 12.4523 [g/cm⁻³]

Luminosity = 0.00734846666 [L_☉]

Luminosity_{DM} = 0.00977020 [L_☉]

TESS Period = nan [days]

Lomb-Scargle Period = 0.5930 ± 2.3444e-07 [days]

wdflag = 0 raddflag = 1

P_{cyc} = 3.4560 ± 0.27091 [years]

Selected active fully convective M-type main-sequence stars

5

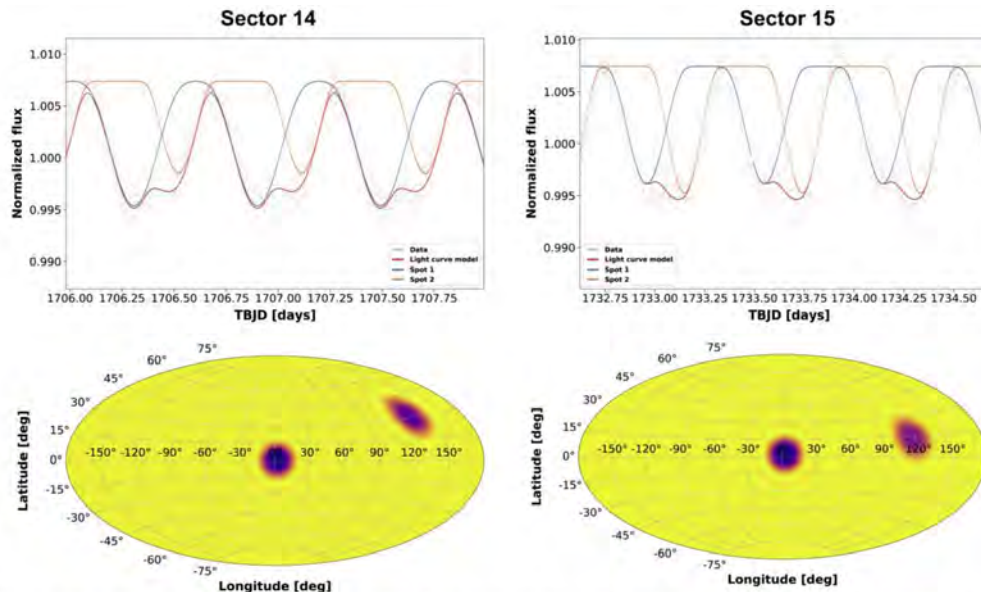


Figure 3. The upper panels show the contribution of each spot to the light curve (the orange and blue curves), the red curves represent the recreated light curve, and the black dots are observations from TESS. The bottom panels present the locations, sizes, and contrasts of the spots in Aitoff projections. The left panels are for sector 14 and the right panels are for sector 15. Both Aitoff projections assume that phase = 0 at TESS Barycentric Julian Date (TBJD) = 1701.78 days.

Table 1
Parameters of the Spots on GJ 1243 in Sectors 14 and 15

Sector Number	Spot Number	Spot Relative Amplitude (%)	Spot Size (% of Area of Star)	Mean Spot Temperature (K)	Spot Latitude (deg)
14	1	0.3 ± 0.01	1.58 ± 0.29	2863 ± 345	31 ± 1
14	2	0.5 ± 0.05	1.75 ± 0.24	2733 ± 464	0 ± 2
15	1	0.4 ± 0.05	1.96 ± 0.28	2882 ± 353	13 ± 3
15	2	0.6 ± 0.06	1.91 ± 0.28	2666 ± 557	1 ± 2

Table 2
Comparison of the Analytically Estimated Spot Parameters and the Ones Achieved by Modeling the Spots on GJ 1243

Sector Number	Analytical Mean Spot Temperature (K)	Model Mean Spot Temperature (K)	Analytical Spot Size (% of Area of Star)	Model Spot Size (% of Area of Star)
14	2876 ± 86	2796 ± 395	3.08 ± 1.08	3.33 ± 0.53
15	2876 ± 86	2782 ± 470	3.21 ± 1.11	3.87 ± 0.56

Bicz et al., 2022

Selected active fully convective M-type main-sequence stars

6

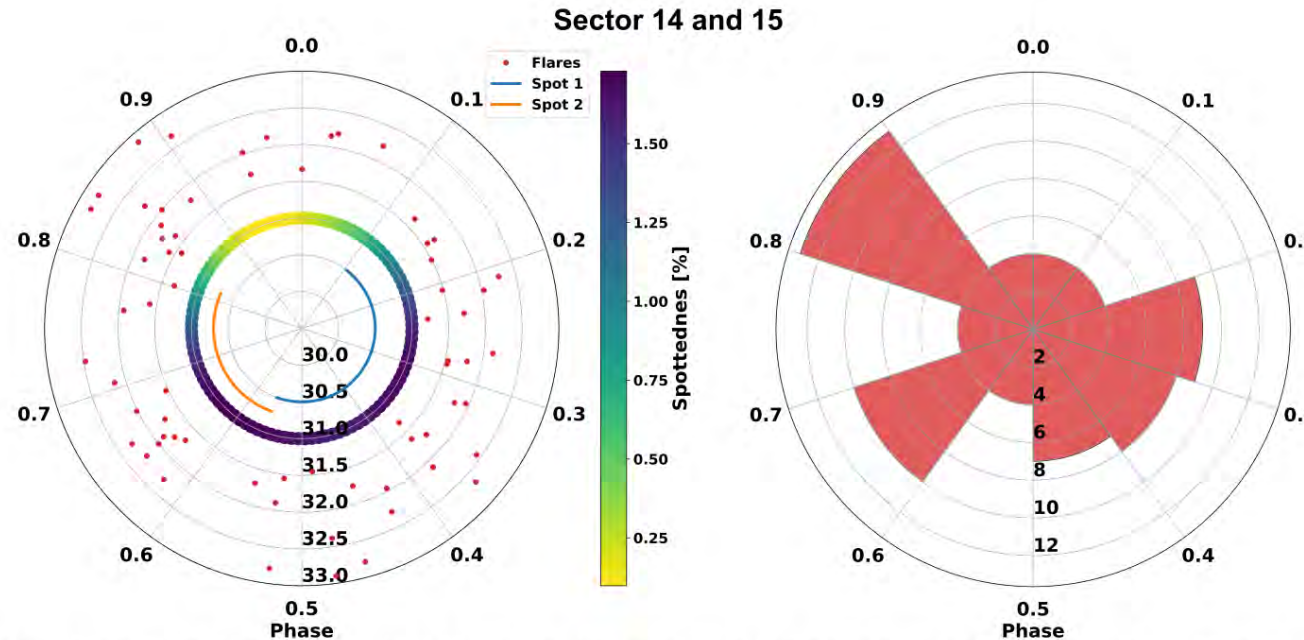


Figure 7. Left panel: the distribution of the bolometric energies of each flare that occurred on GJ 1243 as a function of rotational phase. The orange and blue lines illustrate in which part of the rotational phase a spot was observed on the visible side of the star. The yellow–purple line shows how the visible spottedness changes with phase. The radial axis shows a logarithm of the energy of the flares in ergs. Right panel: the number of flares in 10 equal parts of the rotational phase for GJ 1243. The radial axis marks the number of flares.

Bicz et al., 2022

TIC ID = 266744225 HD = nan V*YZCMi Eruptive*

RA = 116.167385953219 [deg]

DEC = 3.55246606437931 [deg] Canis_Minor

Tmag = 8.33732 [mag] Terr = 0.00743012 [mag] DM = -4.6215 [mag]

SpType = M4.0Ve SpType_{B-V} = K5V_(Pecaut)

Parallax = 167.019 [mas] Parallax err = 0.0591697 [mas] Dist = 5.98632 [parsec]

U = nan [mag] B = 12.38 [mag] V = 11.19 [mag] B-V = 1.190 [mag]

Teff = 3181.0 [K] Teff_{B-V} = 4328 [K]

log(g/[cm · s⁻²]) = 4.89065

Radius = 0.333227 [R_☉] Radius_{DM} = 0.392716 [R_☉]

Mass = 0.31482 [M_☉]

Density = 8.50828 [g · cm⁻³]

Luminosity = 0.010243061 [L_☉]

TESS Period = nan [days]

wdflag = 0 raddflag = 1

Luminosity_{DM} = 0.0141677 [L_☉]

Lomb-Scargle Period = 2.7726 ± 1.7417e-06 [days]

P_{cyc} = 5.0042 ± 0.76547 [years]

Table 1: Parameters of spots on YZ CMi in sector 34 for both light curves.

Observational cadence	Spot number	Spot relative amplitude [%]	Spot size [%]	Mean spot temperature [K]	Spot latitude [deg]
two-min	1	0.20 ± 0.02	1.53 ± 0.03	2912 ± 235	-12 ± 1
two-min	2	0.36 ± 0.01	1.55 ± 0.06	2713 ± 405	50 ± 1
two-min	3	0.56 ± 0.03	2.14 ± 0.05	2696 ± 478	36 ± 0.4
two-min	4	0.49 ± 0.06	2.13 ± 0.06	2756 ± 420	-36 ± 0.4
20-sec	1	0.12 ± 0.032	1.54 ± 0.061	3023 ± 137	-10 ± 4
20-sec	2	0.29 ± 0.024	1.84 ± 0.13	2755 ± 379	51 ± 5
20-sec	3	0.62 ± 0.071	2.18 ± 0.094	2652 ± 518	44 ± 3
20-sec	4	0.39 ± 0.089	1.52 ± 0.11	2800 ± 335	-39 ± 3

Selected active fully convective M-type main-sequence stars

9

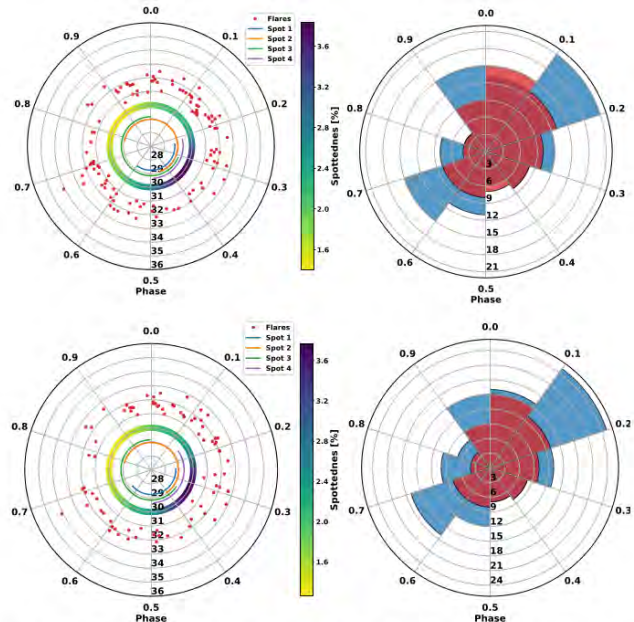


Figure 5. On the left, we compare the flare energies, spottedness, and the visibility of the spots as a function of phase. The orange, blue, green, and purple lines represent the visibility of the spots. The yellow-purple ring shows the visible spottedness. The radial axes present logarithms of the energy of the flares in ergs. Right panels: the number of flares in 10 equal phase sectors for YZ CMi. The number of flares is marked on the radial axis. The upper right panel shows the comparison between flares detected on the two-minute cadence light curve (red histogram) compared with the flares detected on the 20-sec cadence light curve, for which we were able to estimate properly the blue histogram. The bottom right panel shows the comparison between flares detected on the two-minute cadence light curve (red histogram) compared with all of the flares detected on the 20-sec cadence light curve (blue histogram).

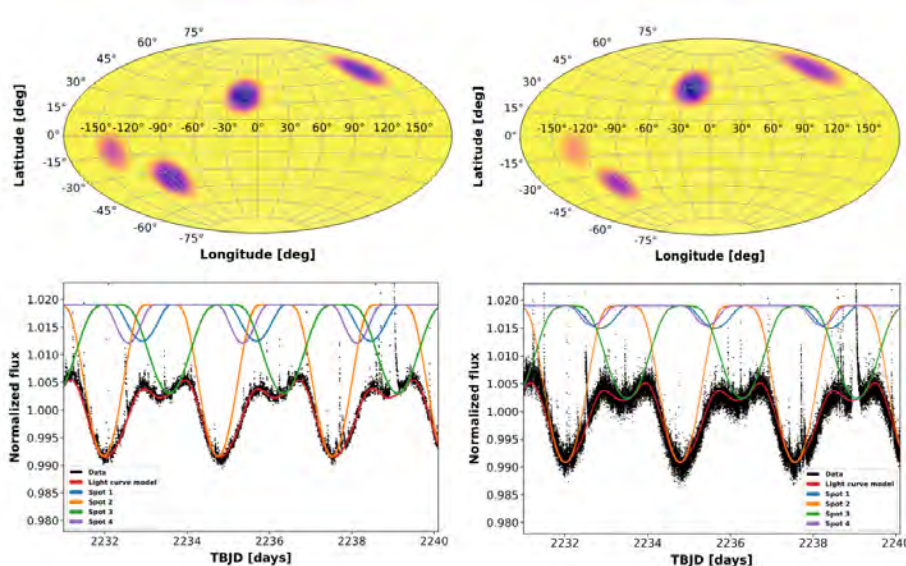


Figure 1: Left panels present the results obtained by analyzing the two-minute cadence light curve. Right panels present the results obtained by analyzing the 20-sec cadence light curve. The upper panels show the locations, sizes, and contrasts of the spots in the Aitoff projection. Figure from the

Selected active fully convective M-type main-sequence stars

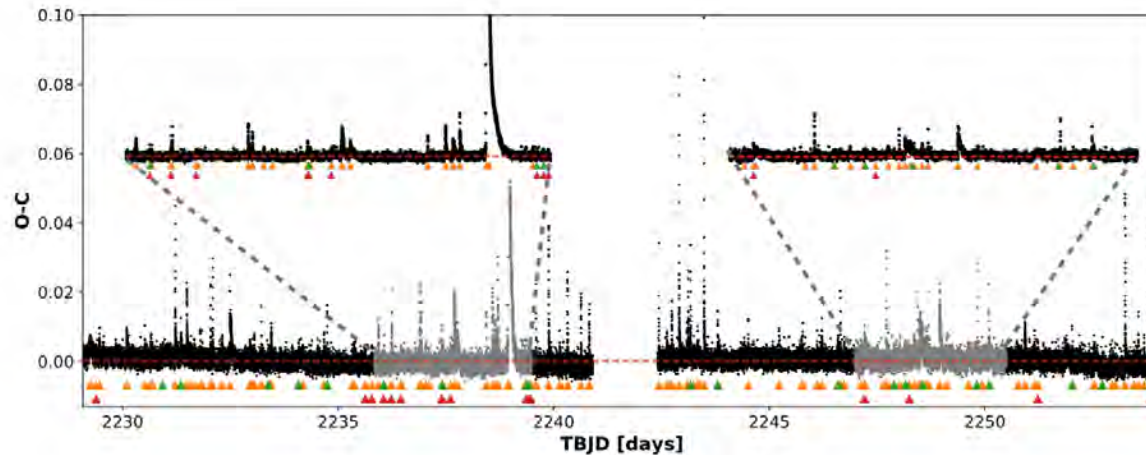


Figure 3: The light curve of YZ CMi (sector 34), corrected for the rotational modulation. The red dashed line presents the zero level. The triangles mark the moments of the energy release maxima for all the detected flares. The newly detected flares after correcting the light curve for rotational modulation are shown in green. Flares, which due to the low SNR, could not have estimated energy properly were marked with red triangles. The gray points mark the fragments of the light curve that the upper part of the graph zooms in on. Figure from the manuscript under preparation.

Selected active fully convective M-type main-sequence stars

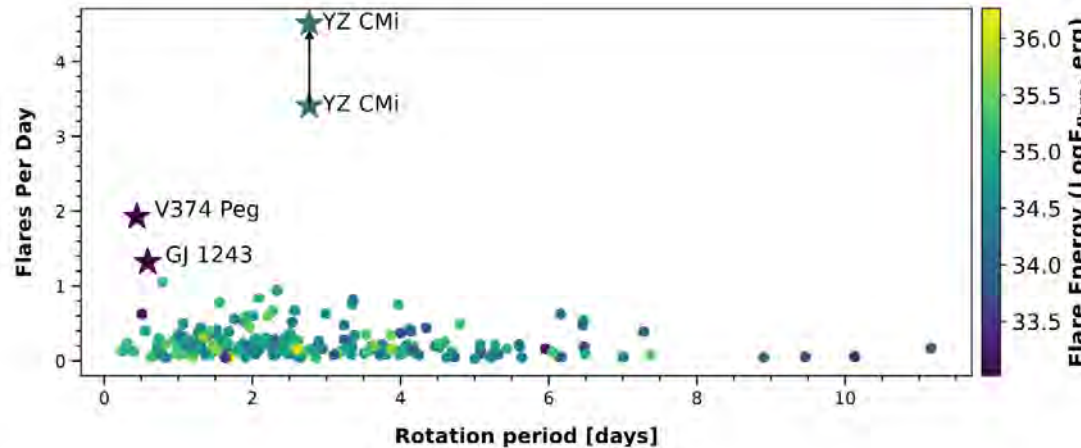


Figure 2: The upper panel presents the number of flares per day for GJ 1243, YZ CMi, V374 Peg (presented as stars) and for stars from Doyle et al. (2020) (presented as points) as a function of the rotation period. The points are color-coded and present the maximum flare energy from the star. The energies are $10^{33.36}$ erg for GJ 1243, $10^{33.63}$ erg for V374 Peg, and $10^{34.62}$ erg for YZ CMi. The black arrow presents the shift in the number of flares per day thanks to the analysis of 20-sec cadence TESS data comparing with the Bicz et al. (2022). Figure from the manuscript under preparation.

CD-36 3202

K2V(e) C

$v\sin(i) = 170 \pm 17$

$T_{\text{eff}} = 4885 \text{ K}$

$\log(g) = 4.53$

$R = 0.8 \text{ R}_{\odot}$

$M = 0.8 \text{ M}_{\odot}$

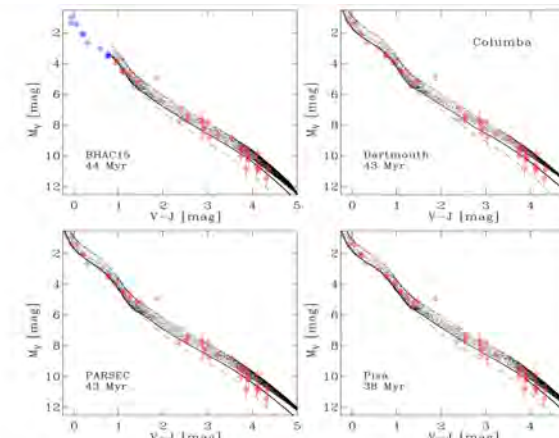
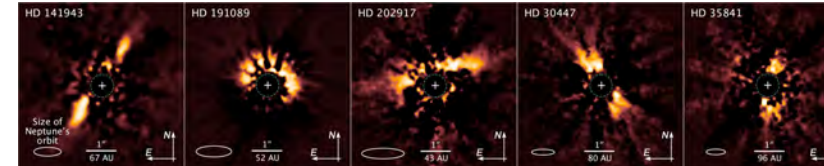
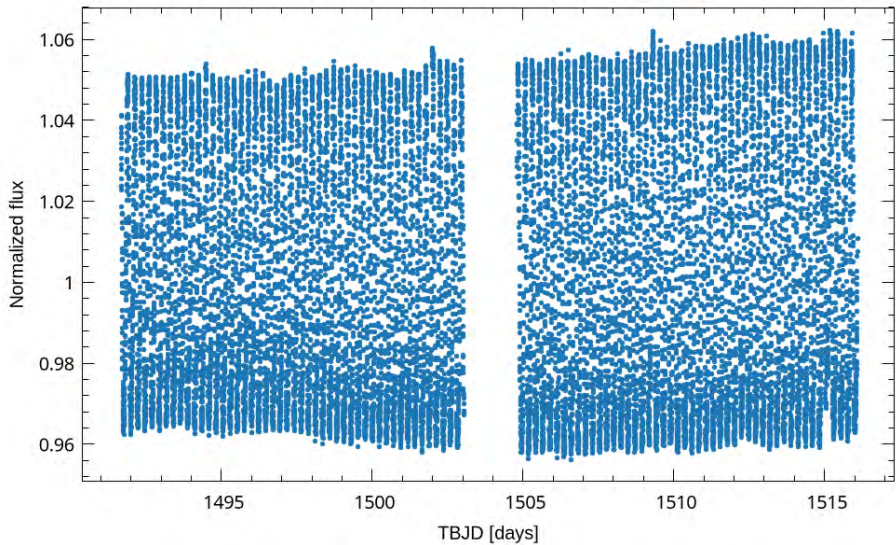
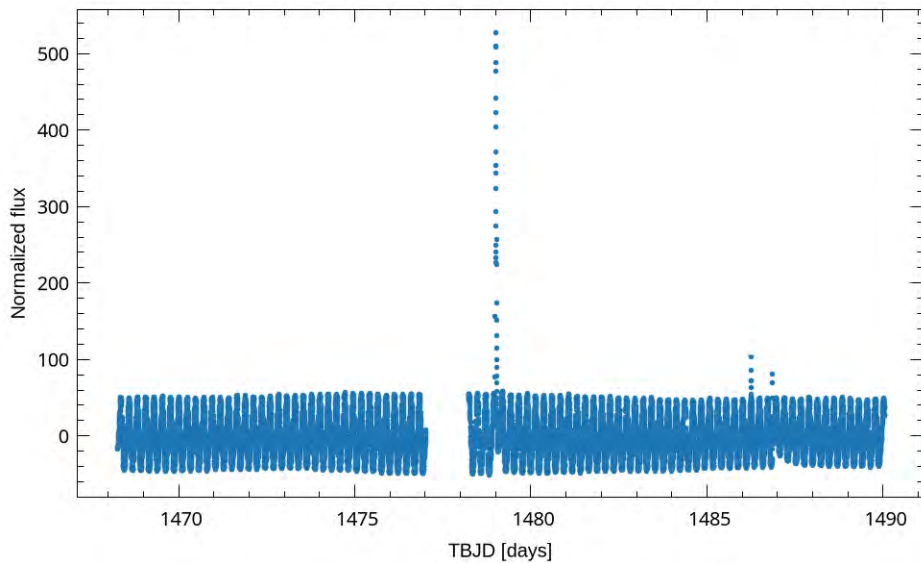


Figure 7. Best-fitting $M_V, V - J$ CMDs of Columba. The coloured symbols and dashed lines are the same as those in Fig. 2: Top left: BHAC15. Top right: Dartmouth. Bottom left: PARSEC. Bottom right: Pisa. Bell et al., 2014

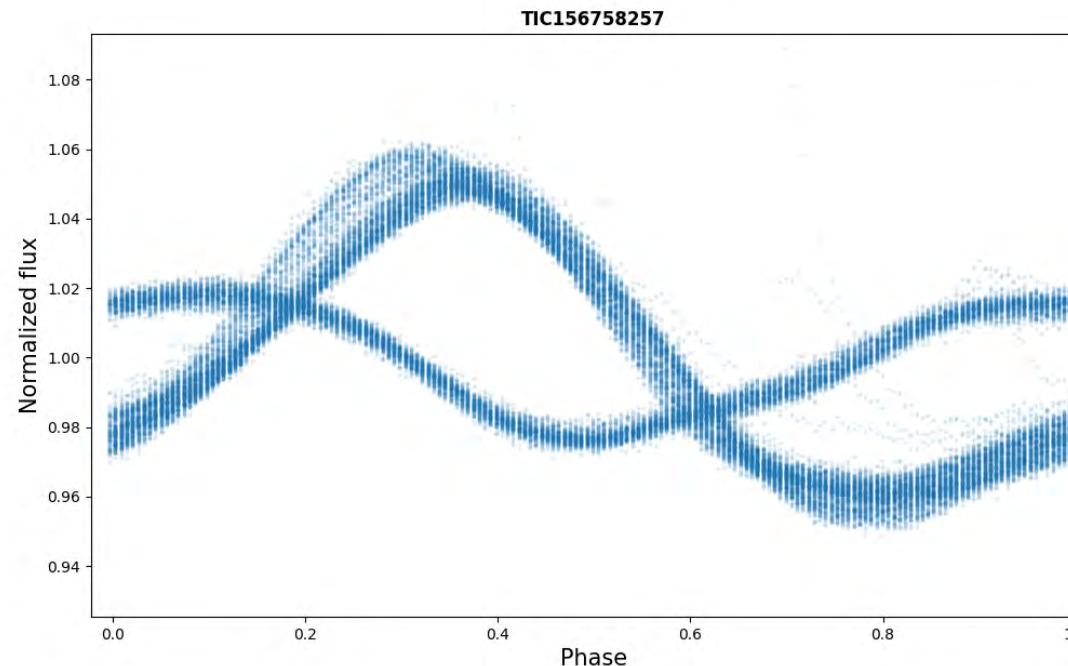
Partially convective star CD-36 3202

13

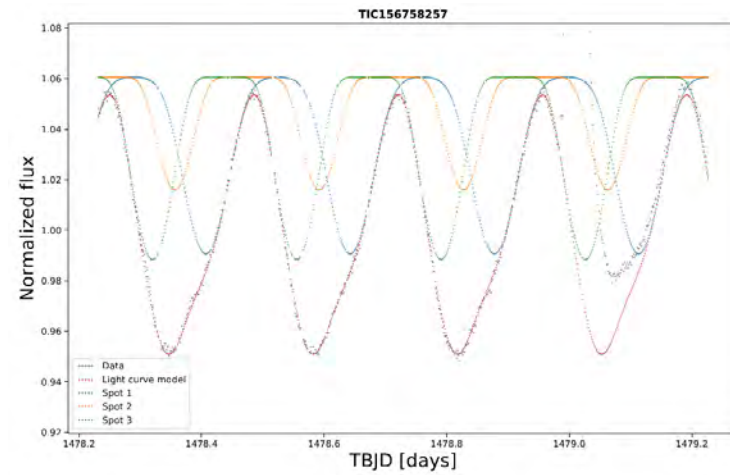
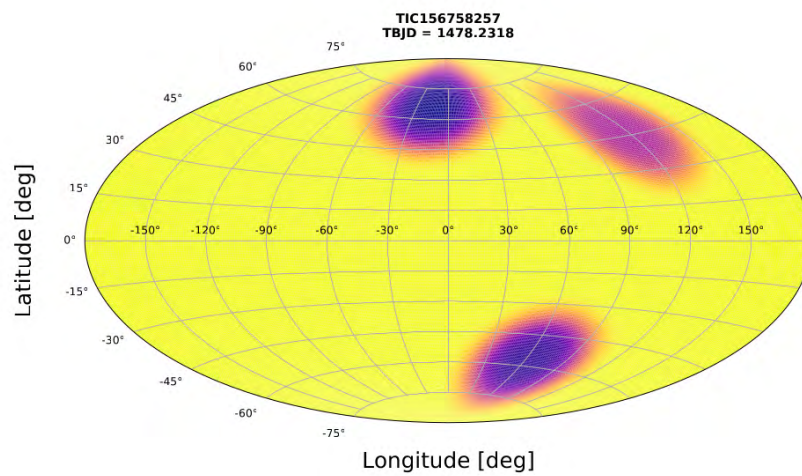


Partially convective star CD-36 3202

14

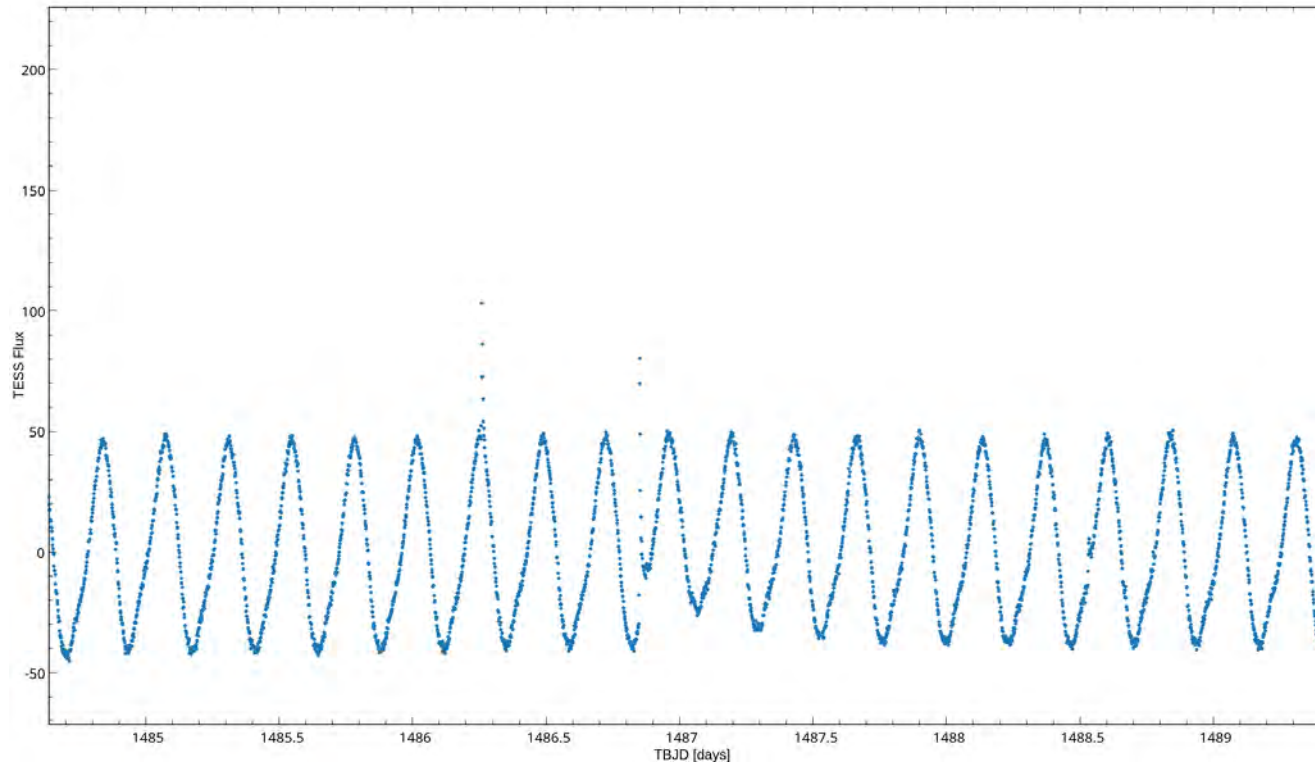


	Amplitude	Size	Latitude	Longitude	Alpha=0.00	Temperature	Size	Radius	Flux
	-	-	[deg]	[deg]	[day]	[K]	[%]	[R*]	[W]
Spot1	-0.09908	0.0488	65.4393	-15.4533	0.2354	3976 ± 1408	4.88203	0.4419	6.92e+05
Spot2	-0.09446	0.0491	-57.1747	61.6299	0.2354	3893 ± 1491	4.90691	0.4430	6.39e+05
Spot3	-0.06082	0.0472	45.9162	117.5498	0.2354	4114 ± 1104	4.72304	0.4347	7.67e+05



Partially convective star CD-36 3202

16



Kamil Bicz, Astronomical Institute of the University of Wrocław

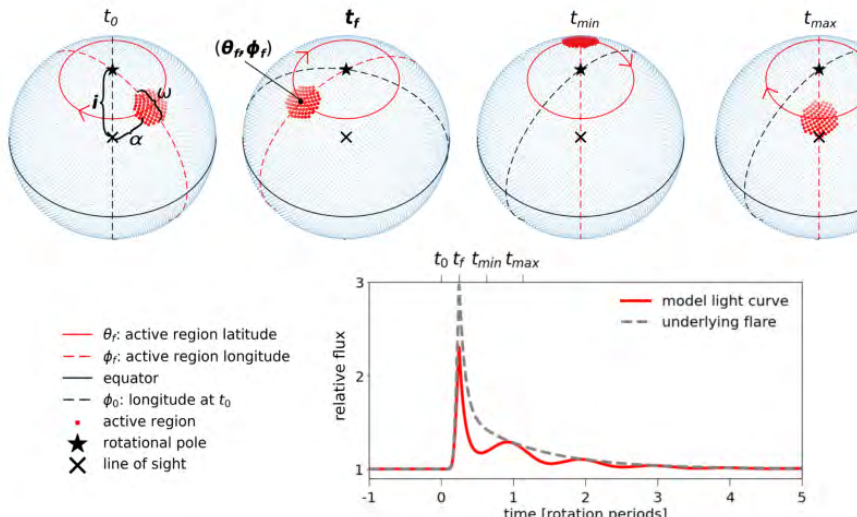


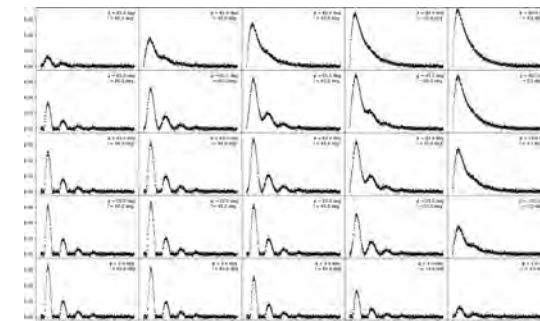
Figure 5. Flare modulation model. From left to right, the top row shows a clockwise rotating star (blue dots) with a flaring region (red dots), from the start of observation at t_0 to the peak flare time t_f , and further to the flaring region being rotated to the stellar far (t_{\min}) and near (t_{\max}) sides. The angular distance between the rotational pole (black star) and the intersection of the line of sight with the centre of the star (black cross) is the inclination i . α is the angular distance of the flaring region to the line of sight, and ω is the full opening angle of the circular flaring region. The depicted configuration results in the observed light curve (red line) in the bottom panel. The underlying flare model is shown as a grey dashed line in the same panel.

Ilin et al., 2021

$$\omega/2 = \arcsin \left(\sqrt{\frac{A \cdot L_*}{\pi R_*^2 F_{f,s}(T_f)}} \right).$$

$$\alpha = \arccos (\sin \theta \cos i + \cos \theta \sin i \cos(\phi - \phi_0 - \hat{i})).$$

$$F_f(\theta, \phi, \hat{t}) = F_f(\hat{t}) \cos \alpha(\theta, \phi, \hat{t}).$$



Partially convective star CD-36 3202

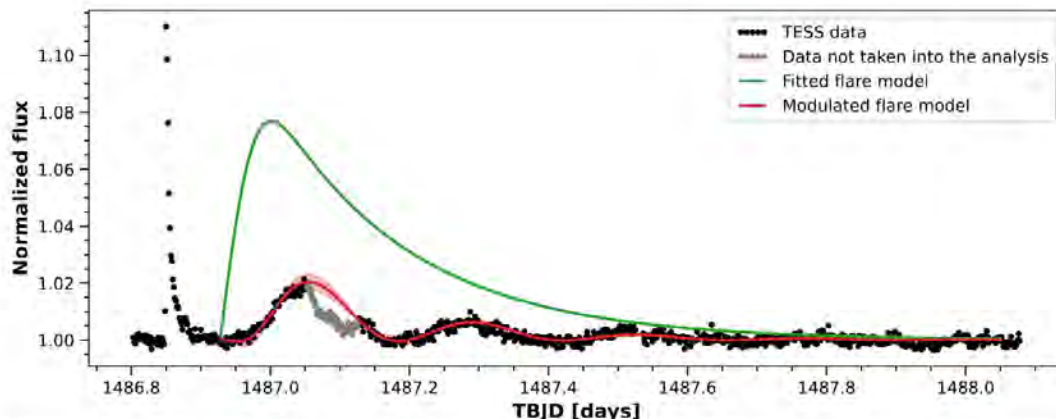


Figure 1. Part of the TESS light curve from sector 6 corrected to the variability caused by stellar spots. The red curve and red interval mark the modulated flare model and the fit error respectively. The green curve shows the recreated course of the stellar flare without the effects of foreshortening and stellar rotation. Gray points mark the data not used in the analysis. The translucent red area presents the uncertainty area.

> Radius = 2.53 deg
> Latitude = 80.35 + 2.55 - 2.48 deg
> Longitude = 205.79 + 2.51 - 2.45 deg

Old energy: $1.15\text{e}35 \pm 3.51\text{e}34$ erg
New energy: $8.81\text{e}35 \pm 2.68\text{e}34$ erg

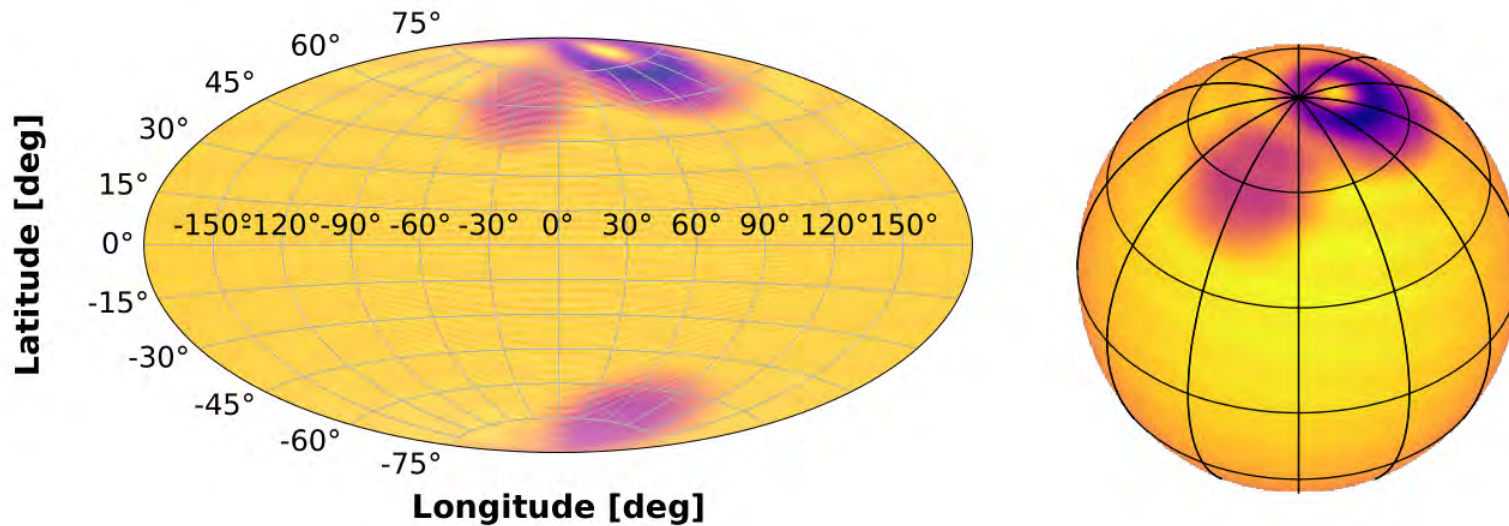
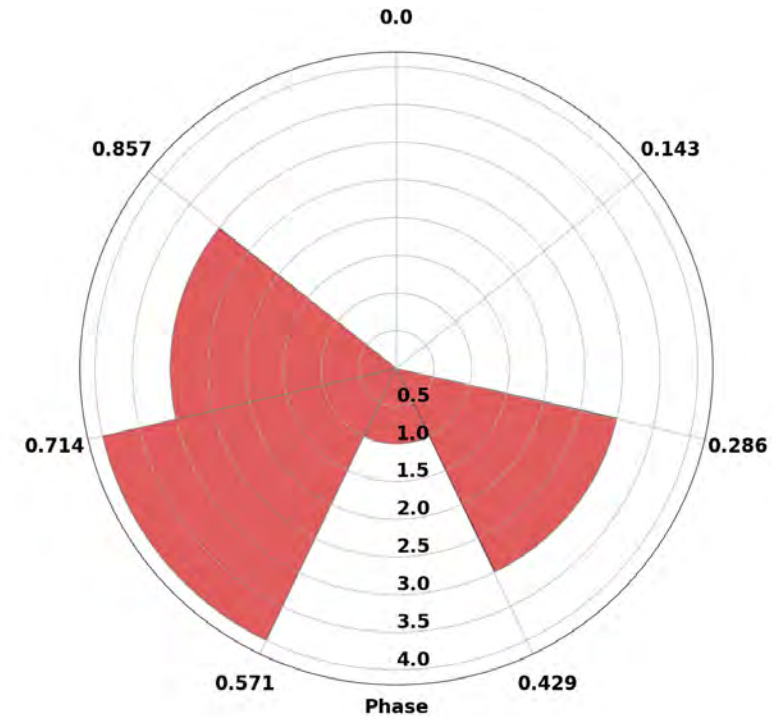
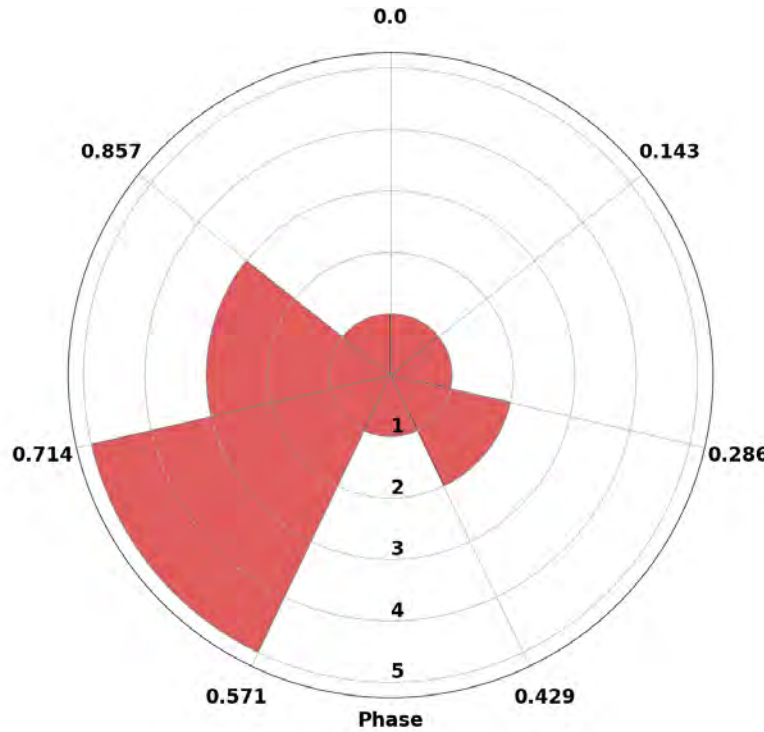


Figure 2. Both panels show the average distribution of starspots on the star CD-36 3202 in sector 6. The bright region on the latitude approximately 80° and longitude approximately 100° is the flare from Figure 1. The left panel presents the star in the Aitoff projection and the right panel presents the model of the star in the orthographic projection. Figure from the manuscript under preparation.





Thank you for your attention!

Kamil Bicz
bicz@astro.uni.wroc.pl
Astronomical Institute
University of Wrocław
Kopernika 11, 51-622 Wrocław, Poland

Bezovec
June 17, 2023